

# Multi-Level Library of Electrical Machines for Aerospace Applications

P. Giangrande      C.I. Hill      C. Gerada      S.V. Bozhko  
University of Nottingham  
PEMC Group, Nottingham, NG7 2RD, UK.  
p.giangrande@nottingham.ac.uk      c.hill@nottingham.ac.uk

## Abstract

An electrical machine library, developed within the framework of the European project *Actuation 2015*, is presented in this paper. The library has been developed adopting a multi-level approach, in order to minimize the models complexity and reduce the computational time. Multi-level approach consists in creating several models of the same electrical machine topology, with different levels of complexity. Indeed, model complexity increases at higher model levels and each model takes into account specific physical effects. In addition to the fundamental behavior, the presented models address physical effects such as losses, magnetic saturation, torque ripple and fault conditions. The interchangeability among model levels is ensured by using common interfaces. An overview of the library structure is given; however, particular attention is paid on the permanent magnet synchronous machine (PMSM) models, since they are becoming increasingly widespread in aerospace applications. The PMSM models description and simulation results are provided, in order to highlight the implemented physical effects and confirm the models effectiveness.

*Keywords: Permanent Magnet Synchronous Machine, Multi-Level, Losses, Magnetic Saturation, Torque Ripple, Fault conditions.*

## 1 Introduction

According to the concept of the More Electric Aircraft (MEA), an increasing number of hydraulic actuators for primary and secondary flight control surfaces are being replaced by Electromechanical Actuators (EMAs), in order to improve efficiency, weight and maintenance of the aircraft [1]. For this reason, EMAs are becoming an attractive research area and part of the research work is focused on developing virtual testing environments and analysis tools. Indeed, EMAs' manufacturers require simulation tools capable of analyzing EMAs performance and exploring different design configurations. In response to

these requirements, a suitable simulation and analysis tool for EMAs, named *Actuator* library, has been developed within the framework of the European project *Actuation 2015*.

The multidisciplinary architecture of EMAs could lead to a large simulation time or even numerical non-convergence due to the model complexity [2]. In order to avoid these issues, the idea of implementing several models of the same component (i.e.: inverter, electrical machine, gear box etc...), with different levels of complexity has been exploited. Hence, a multi-level approach has been adopted, with the aim of keeping the models as simple as possible, since a good model is a wise trade-off between realism and simplicity.

The model levels are categorized by the complexity of the physical effects implemented within the model. In particular, higher model levels take into account more complex physical effects. Considering that several models of the same component are available within the library, the interchangeability among the model levels is crucial, in order to investigate different physical effects by simply replacing the model level. For this reason, the interchangeability has been ensured by using common interfaces among the model levels.

In this paper, the *Electrical Machines* library, which is part of the *Actuator* library, is presented. The *Electrical Machines* library has been implemented using Modelica [3], as modelling language, and Dymola, as simulation environment. This library is organized as three packages and each of them considers a specific machine topology, such as PMSM, synchronous reluctance machine (SRM) and direct current (DC) machine. Each one of these packages contains the sub-package *Examples*, which provides several case studies, helpful for highlighting the features of each modelling level. Due to space constraints, not all the machine topologies included in the *Electrical Machines* library will be considered in this paper. Indeed, the presented work is mainly focused on describing the

PMSM models as these machines are characterized by an excellent efficiency, together with a high power density [4]. These features make PMSMs very attractive for aerospace applications [5]. Whilst initially resistance to the adoption of these machines was shown by airframes to the possibility of unsuppressed short-circuit currents, it is now more accepted that through fault tolerant design and health monitoring schemes these machines offer an optimum solution.

In the next sections, an overview of the `Electrical Machines` library is presented along with a description of the model interfaces. Moreover, details of the PMSM modelling levels and the physical effects (i.e.: losses, magnetic saturation, torque ripple and fault conditions), taken into account, are given. Simulation results obtained using Dymola are also included.

## 2 Library Structure

An overview of the `Electrical Machines` library is provided in this section and figure 1 shows the library structure.

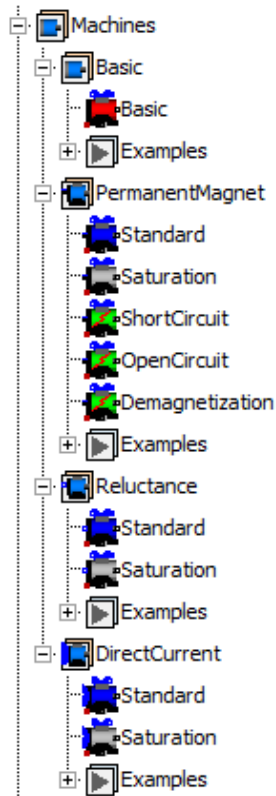


Figure 1: Structure of the `Electrical Machines` library as part of the `Actuator` library.

The machines considered in this library are PMSM, SRM and DC machine. The PMSM type covers a number of topologies from non-salient surface mount to high reluctance interior permanent magnet (IPM) machines. The library is organized in three packages,

one for each machine topology earlier mentioned, plus the package `Basic`, which considers a generic alternating current (AC) electrical machine. According to the multi-level approach previously introduced, several models with different level of complexity are included within each of the four packages. The level of complexity is related with the physical effects that the model takes into account. In other words, a higher level of complexity implies the modelling of more complex physical effects, such as non-linear effects.

The package `Basic` contains only one model level (model `Basic`), which is the simplest model for an AC electrical machine. Indeed, model `Basic` is defined by means of the torque constant and its behavior is ideal (losses and non-linear effects are neglected). Package `PermanentMagnet` includes the three-phase PMSM models and three model levels, such as `Standard`, `Saturation` and `Fault` models, are provided. Three-phase SRM models are organized in the package `Reluctance` and two model levels (`Standard` and `Saturation`) are implemented. Finally, the package `DirectCurrent` considers the DC machine models with independent excitation. This package consists of two modelling levels (`Standard` and `Saturation`). As previously underlined, the sub-package `Examples` is provided for each of the mentioned packages, in order to support the user in both familiarizing with the models and exploring their features.

It is worthy to remark that the contribution of this work is mainly focused on the package `PermanentMagnet` and all the considerations presented in the coming sections are made considering PMSM.

## 3 Models Interfaces

As mentioned earlier, every model belonging to a level is replaceable with one belonging to another level. This feature has been achieved by adopting common interfaces, which are defined in `Actuator.Electrical.Interfaces`. The adopted model interfaces can be classified according their function in:

- electrical interface;
- mechanical interface;
- thermal interface.

All quantities accessible at the mentioned interfaces are shown in physical units.

Considering AC electrical machines (packages `Basic`, `PermanentMagnet` and `Reluctance`), the electrical interfaces adopted are the `PositivePlug` and `NegativePlug`, since the stator winding is assumed as three-phase winding. In particular,

the AC machine models have been built up considering a wye-connected stator winding, with floating neutral point. The adopted electrical interfaces allow connecting the AC machine to a power converter or to a driven voltage source (`SignalVoltage`). In the case of the DC machine models, `PositivePin` and `NegativePin` have been used as electrical interfaces, for both armature and field windings (the DC machine excitation is independent).

All the machine models adopt `Flange` and `Support` as mechanical interfaces and they are included in the models by extending the `PartialOneFlangeAndSupport`. The developed electromagnetic torque and the load torque are applied on the machine `Flange`, while the reaction torque is available on the `Support`, in case the machine housing is not grounded.

The `PartialConditionalHeatPort` is used as thermal interface for all the machine models and housing temperature and heat flow are available at the heat port.

## 4 Model Basic

The model `Basic` is included in the package `Basic` and it is the simplest model for a generic three-phase AC machine. The machine behavior is described through the torque constant, which establishes the relationship between current and electromagnetic torque. Copper, iron and mechanical losses are not considered at this level, as well as, effects such as magnetic saturation, torque ripple and fault conditions are neglected.

Data records have been used to organize the model parameters and for the model `Basic` the required parameters are:

- Phase resistance ( $R$ );
- Magnetizing inductance ( $L$ );
- Pole pairs number ( $pp$ );
- Torque constant ( $k_t$ );
- Rotor's moment of inertia ( $J_r$ );
- Stator's moment of inertia ( $J_s$ ).

The stator's moment of inertia will be used by the model only when the machine housing is not grounded. Since plugs are used as electrical interfaces, the model `Basic` is fed using phase quantities ( $abc$ ) and Park's transformation (invariant amplitude transformation) [6] is adopted for implementing the model in the rotating reference frame ( $dq$ ), according to the following equations:

$$\begin{aligned} v_d &= R \cdot i_d + L \cdot \frac{d}{dt} i_d - \omega_e \cdot L \cdot i_q \\ v_q &= R \cdot i_q + L \cdot \frac{d}{dt} i_q + \omega_e \cdot L \cdot i_d + \frac{2 \cdot k_t}{3 \cdot pp} \cdot \omega_e \end{aligned} \quad (1)$$

where  $\omega_e$  is the electrical speed in  $rad/s$ . The electromagnetic torque ( $\tau_e$ ) developed by the model `Basic` is given by:

$$\tau_e = k_t \cdot i_q \quad (2)$$

The electrical equations are implemented in the *Modelica Text Layer*, while the mechanical model is realized in the *Modelica Diagram Layer*, using an object-oriented approach. In figure 2, the *Modelica Diagram Layer* of the model `Basic` is shown. Model `Basic`, as well as all the other machine models presented in the `Electrical Machines` library, is reversible. This means that the model `Basic` can work reversibly as motor or generator.

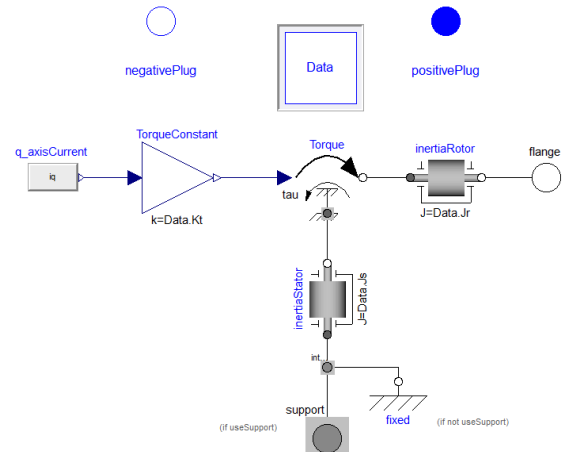


Figure 2: *Modelica Diagram Layer* of the model `Basic` included in the `Electrical Machines` library.

In order to verify the model `Basic` functionality, the simple EMA architecture, reported in figure 3, has been implemented and simulated in Dymola. The chosen EMA architecture consists of an inverter, which supplies a PMSM mechanically coupled to a 500  $rad/m$  transmission ratio roller screw, through a gearbox with transmission ratio equal to 5. The inverter is fed using a 270 V DC link and the PMSM parameters are: 14 pole pairs, 56.2  $g \cdot m^2$  rotor inertia, 0.05  $\Omega$  phase resistance, 2 mH magnetizing inductances and 2.1  $Nm/A$  torque constant. Control unit (*controller*) implements the conventional position control, hence the position is controlled by a cascaded structure, where the inner loop controls the  $q$ -axis current, the outer loop controls the speed and finally the outermost loop controls the position. During the simulation, the controlled sur-

face is moving 0.02  $m$  forward and backward, while an external load force of -80000  $N$  (equivalent to -32  $Nm$  load torque on the PMSM shaft) is acting on the flight surface. The simulation results are shown in figure 4. In particular the mechanical quantities (position, speed and torque) of the PMSM are reported and a good agreement between actual and reference position is highlighted.

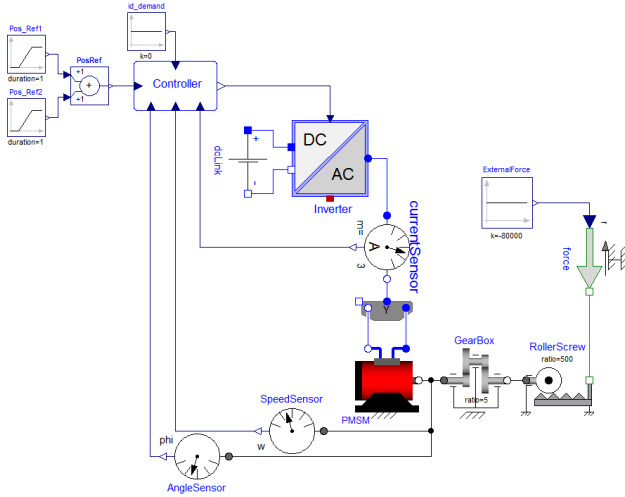


Figure 3: EMA architecture simulated in Dymola, using the model Basic.

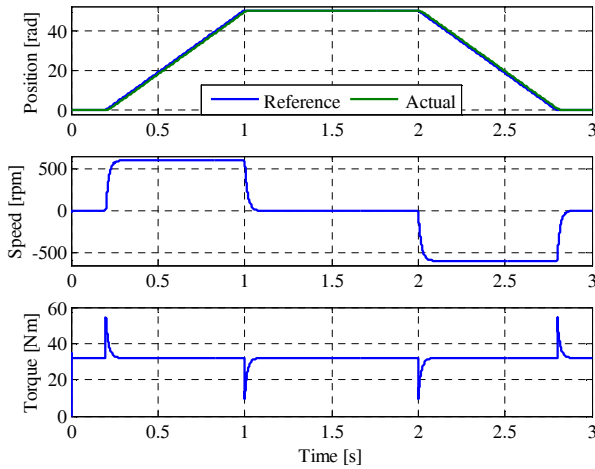


Figure 4: Simulation results obtained using the model Basic under position control: mechanical rotor position (top), mechanical rotor speed (middle) and developed torque (bottom).

## 5 Model Standard

The model Standard, included in the package PermanentMagnet, is based on a lumped parameters approach and it describes the behavior of PMSMs taking into account torque generation, losses and thermal model. Non-linear effects, such as magnetic saturation, torque ripple and fault conditions are neglecting at this level.

The model is developed in the rotating reference frame synchronous with the rotor ( $dq$ ) and Park's transformation (invariant amplitude transformation) is used to pass from the  $abc$  to the  $dq$  reference frame. Figure 5 reports the equivalent circuits in the rotating reference frame.

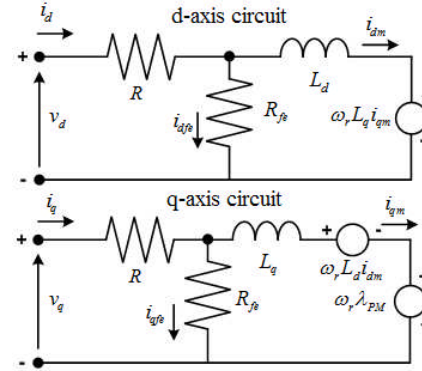


Figure 5:  $d$  – and  $q$  – axis equivalent circuits implemented within the model Standard.

These equivalent circuits take into account the iron losses using an equivalent iron losses resistance ( $R_{fe}$ ), placed in parallel with the series between the magnetizing branch and the electromotive force term [7]. Applying the Kirchhoff's voltage law (KVL) at the main loop of the circuits in figure 5, the following equations can be written:

$$v_d = R_t \cdot i_d + L_d \cdot \frac{d}{dt} i_{dm} - \omega_e \cdot L_q \cdot i_{qm} \quad (3)$$

$$v_q = R_t \cdot i_q + L_q \cdot \frac{d}{dt} i_{qm} + \omega_e \cdot L_d \cdot i_{dm} + \omega_e \cdot \lambda_{pM}$$

where  $R_t$  is the phase resistance (which is function of the winding temperature),  $\lambda_{pM}$  is the permanent magnet flux,  $L_d$  and  $L_q$  are the  $d$  – and  $q$  – axis magnetizing inductances respectively. These parameters ( $R$ ,  $L_d$ ,  $L_q$  and  $\lambda_{pM}$ ) are provided by the model user, through the model's mask. On the other hand, applying the Kirchhoff's current law (KCL) at the circuit nodes results:

$$\begin{aligned} i_d &= i_{dfe} + i_{dm} \\ i_q &= i_{qfe} + i_{qm} \end{aligned} \quad (4)$$

According (4), the total currents ( $i_d$  and  $i_q$ ) are split into iron losses currents ( $i_{dfe}$  and  $i_{qfe}$ ), given by (5), and magnetizing currents ( $i_{dm}$  and  $i_{qm}$ ). The formers flow through the equivalent iron losses resistance, while the latter are responsible of the torque generation.

$$\begin{aligned} i_{dfe} &= \left( L_d \cdot \frac{d}{dt} i_{dm} - \omega_e \cdot L_q \cdot i_{qm} \right) / R_{fe} \\ i_{qfe} &= \left( L_q \cdot \frac{d}{dt} i_{qm} + \omega_e \cdot L_d \cdot i_{dm} + \omega_e \cdot \lambda_{PM} \right) / R_{fe} \end{aligned} \quad (5)$$

In order to complete the PMSM model, the electromagnetic torque equation has to be explicit. In general, the torque developed by the PMSM is the sum of two terms: the field torque due to the permanent magnets and the reluctance torque due to the machine saliency. PMSM model Standard includes both these torque terms, hence the behavior of surface mounted (SMPM) and interior permanent magnet (IPM) machines can be simulated. The electromagnetic torque is given by (6):

$$\tau_e = \frac{3}{2} \cdot pp \cdot \left[ \lambda_{PM} \cdot i_{qm} + (L_d - L_q) \cdot i_{dm} \cdot i_{qm} \right] \quad (6)$$

where  $pp$  is the pole pairs number, which is provided by the model user.

Model Standard is a power balanced model and the losses taken into account are copper, iron and mechanical losses. Copper losses ( $P_{cu}$ ) are a function of the current and the winding resistance, according to the following equation:

$$P_{cu} = \frac{3}{2} \cdot R_t \cdot (i_d^2 + i_q^2) \quad (7)$$

The coefficient  $3/2$  arises from the adoption of the amplitude invariant Park's transformation. As previously said, the phase resistance  $R_t$  is function of winding temperature ( $\theta_w$ ), through the equation:

$$R_t = R \cdot \left[ 1 + \alpha \cdot (\theta_w - \theta_{ref}) \right] \quad (8)$$

where  $R$  is the phase resistance at the reference temperature ( $\theta_{ref}$ ) and  $\alpha$  is linear temperature coefficient, which depends on the winding material (i.e. copper or aluminum).

Iron losses ( $P_{fe}$ ), both hysteretic and eddy current, are a function of voltage and frequency as well as the material composition. These losses are calculated as equivalent copper losses:

$$P_{fe} = \frac{3}{2} \cdot R_{fe} \cdot (i_{dfe}^2 + i_{qfe}^2) \quad (9)$$

Equivalent iron losses resistance is obtained considering the specific iron losses ( $C_p$ ) and the stator mass ( $m_s$ ):

$$R_{fe} = \frac{(2 \cdot \pi \cdot 50)^2 + \lambda_{PM}^2}{C_p \cdot m_s} \quad (10)$$

Both these parameters ( $C_p$  and  $m_s$ ) are provided by the model user, using the model's mask. Specific iron losses gives the iron losses in 1 Kg mass of a given magnetic material, when it is subject to a flux density of 1 Wb/m<sup>2</sup> at 50 Hz.

Finally, mechanical losses ( $P_{mec}$ ), due to friction and windage, are functions of rotor speed and they are included in the model using the equivalent viscous friction torque ( $\tau_f$ ):

$$\tau_f = B \cdot \frac{\omega_e}{pp} \quad (11)$$

$$P_{mec} = \tau_f \cdot \frac{\omega_e}{pp} \quad (12)$$

where  $B$  is the friction coefficient. The stray losses are neglected in the model Standard, due to their small amount compared to the other losses.

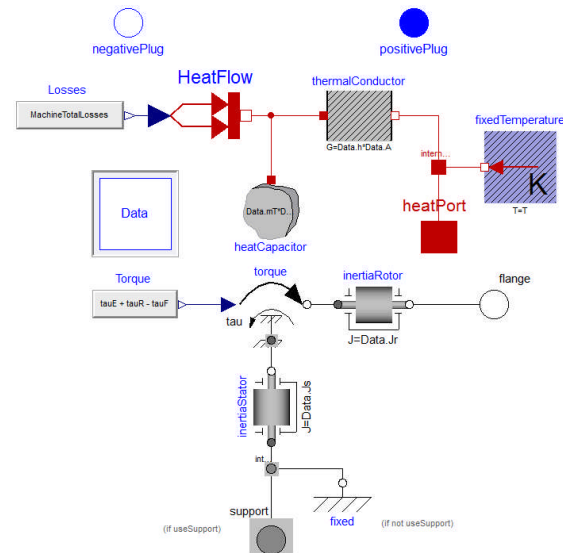


Figure 6: Modelica Diagram Layer of the model Standard included in the Electrical Machines library.

Total losses are applied in input to the thermal model adopting the component PrescribedHeatFlow. The implemented thermal model considers the PMSM as a whole block and it is composed by a heat capacitor and a thermal conductor. The heat capacity ( $C$ ) is defined as:

$$C = c_p \cdot m_T \quad (13)$$

where  $m_T$  is the total motor mass and  $c_p$  is the equivalent specific heat capacity, which depends by the motor materials (mainly copper and iron). However, the convective thermal conductance ( $G$ ) between windings and housing is given by:

$$G = h \cdot A \quad (14)$$



where  $A$  is the convection area and  $h$  is the heat transfer coefficient, which depends upon the cooling system adopted. Both these parameters, together with  $m_T$  and  $c_p$  are provided by the model user. The winding and housing temperatures are respectively available on `port_a` and `port_b` of the thermal conductor. Finally, the heat flow is available at the heat port of the thermal model (`heatPort`). Equations (3)-(14) are implemented in the *Modelica Text Layer*, while the mechanical and thermal models are included in the *Modelica Diagram Layer*, as shown in figure 6.

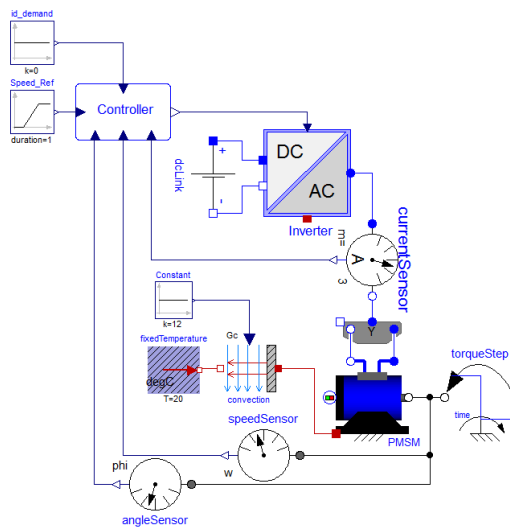


Figure 7: Speed control scheme simulated in Dymola, using the model Standard.

Model Standard has been simulated under speed control using the block diagram reported in figure 7, with the purpose of highlighting the PMSM losses and the thermal behavior. The PMSM parameters are:

- pole pairs number 14;
- rotor's moment of inertia  $56.2 \text{ g} \cdot \text{m}^2$ ;
- phase resistance  $0.05 \text{ } \Omega$ ;
- $d$  – and  $q$  – axis inductance  $2 \text{ mH}$ ;
- permanent magnet flux  $0.1 \text{ Wb}$ ;
- specific iron losses  $1.1 \text{ W/kg}$  (M300);
- stator mass  $3 \text{ kg}$ ;
- friction coefficient  $0.0002 \text{ Nm} \cdot \text{s}$ ;
- motor mass  $5 \text{ kg}$ ;
- specific heat capacity  $424 \text{ J/(kg} \cdot \text{K)}$ ;
- convection area  $0.75 \text{ m}^2$ ;
- heat transfer coefficient  $12 \text{ W/(K} \cdot \text{m}^2)$ .

During the simulation, the mechanical speed reference signal is a ramp from  $0 \text{ rpm}$  (at  $0.01 \text{ s}$ ) to  $1500 \text{ rpm}$  (at  $1.01 \text{ s}$ ), while the  $d$  – axis current

reference signal is kept equal to  $0 \text{ A}$ . Once the speed reaches the steady state value ( $1500 \text{ rpm}$ ), a load torque step of  $-25 \text{ Nm}$  is applied at  $1.5 \text{ s}$ . Figure 8 shows the PMSM losses (copper, iron and mechanical losses) together with the electrical and mechanical powers. In steady state, the machine efficiency is equal to  $93.45\%$ .

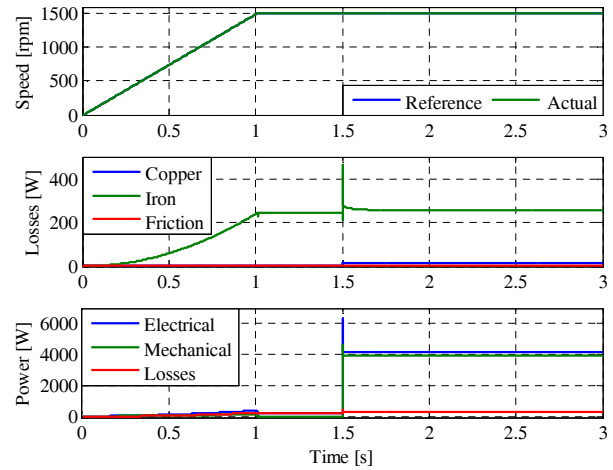


Figure 8: Simulation results obtained using the model Standard under speed control: mechanical rotor speed (top), PMSM losses (middle) and PMSM power (bottom).

The trends of the windings and housing temperatures, over a working period of  $1 \text{ hr}$ , are reported in figure 9.

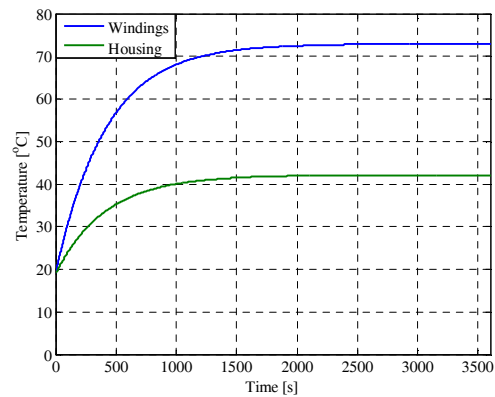


Figure 9: Simulation results obtained using the model Standard: winding and housing temperatures.

## 6 Model Saturation

The model Saturation, included in the package PermanentMagnet, has been obtained as an extension of the model Standard. Therefore it takes into account all the physical effects already presented in the model Standard section, plus the magnetic saturation and the torque ripple. As with the model Standard, the model Saturation is also developed in the rotating reference frame ( $dq$ ) and Park's transformation (amplitude invariant trans-

formation) is used to pass from the  $abc$  to the  $dq$  reference frame.

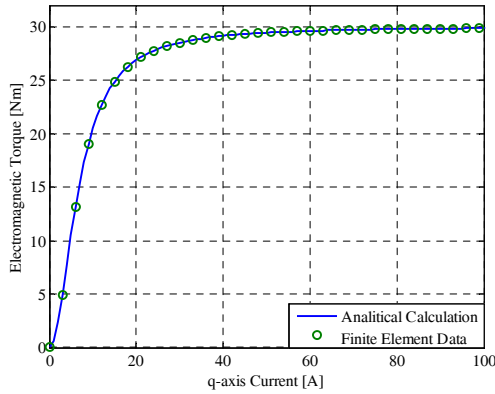


Figure 10: Field torque component against  $q$ -axis current: analytical curve (blue line) and finite element results (green dots).

In ferromagnetic materials, the relationship between the field strength and flux density is not a straight line (i.e. constant permeability), but it is defined through the magnetization curve. Since ferromagnetic materials reveal a variable permeability according to the field strength, the magnetization curve has a knee point. Past this knee point, further increases in the field strength do not result in proportional increases in flux density. The PMSM performance is affected by the magnetic saturation; in particular, it influences both the permanent magnet flux and the inductances. Since the permanent magnet flux and the inductances are a function of the operating point, the developed torque (both field and reluctance terms) is not proportional to the current anymore.

In the model Saturation for PMSM, the magnetic saturation is taken into account considering only its influence on field torque term (i.e. permanent magnet flux), while the reluctance torque term (i.e. magnetic saliency) is not affected by the magnetic saturation. In the presence of magnetic saturation, the curve of the field torque term against the  $q$ -axis current (torque-current curve) has a trend, like shown in figure 10. The torque-current curve can be included in the model Saturation using two approaches:

- the look-up table;
- three given points, which identify the torque-current curve.

In the former case, the data stored inside the look-up table may be obtained by finite element simulations. In the latter case, the model user provides the following data:

- $q$ -axis current at the knee of the torque-current curve ( $I_{qm\text{knee}}$ );

- field torque at the knee of the torque-current curve ( $T_{\text{knee}}$ );
  - field torque at the saturated region of the torque-current curve ( $T_{\text{sat}}$ );
- and the developed torque is analytically calculated using (15).

$$\tau_e = \frac{\sqrt{c_1 \cdot i_{qm}^4 + i_{qm}^2}}{c_2 + i_{qm}^2} \quad (15)$$

where  $i_{qm}$  is the actual magnetizing current along the  $q$ -axis, while  $c_1$  and  $c_2$  are the torque function coefficients. These coefficients are expressed as shown below.

$$c_1 = T_{\text{sat}} \quad (16)$$

$$c_2 = \sqrt{\frac{I_{qm\text{knee}}^4 \cdot T_{\text{sat}}^2 + I_{qm\text{knee}}^2 - I_{qm\text{knee}}^2 \cdot T_{\text{knee}}}{T_{\text{knee}}}} \quad (17)$$

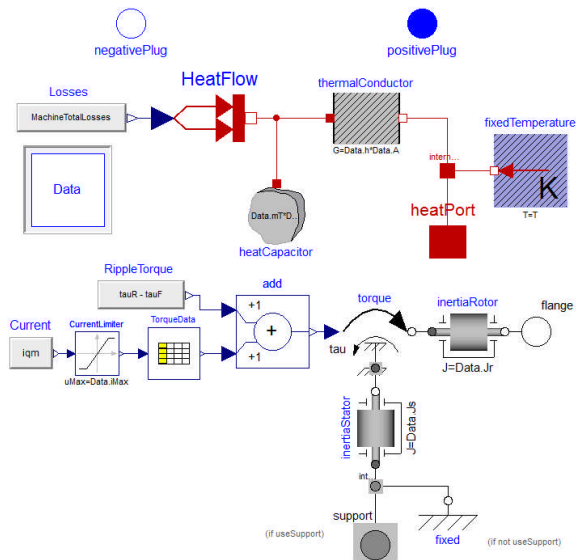


Figure 11: Modelica Diagram Layer of the model Saturation included in the Electrical Machines library.

In addition to the magnetic saturation, the model Saturation, also implements the torque ripple, which is function of the electrical rotor position ( $\vartheta_e$ ). In particular, the model Saturation allows to superimpose a sinusoidal torque ripple ( $\tau_{\text{ripple}}$ ) on the developed electromagnetic torque ( $\tau_e$ ). The torque ripple waveform is defined according (18).

$$\tau_{\text{ripple}} = A_{\text{ripple}} \cdot \sin\left(\frac{f_{\text{ripple}}}{f_n} \cdot \vartheta_e\right) \quad (18)$$

where  $A_{\text{ripple}}$  is the ripple amplitude,  $f_{\text{ripple}}$  is the ripple frequency and  $f_n$  is the PMSM rated frequency. These parameters are provided by the model user by

means of a dedicated mask.  $A_{ripple}$  and  $f_{ripple}$  are function of [8]:

- stator winding (concentrated or distributed, single or double layer);
- motor geometry (slot opening, tooth shape, etc...);
- air-gap flux density quality (harmonic content);
- load conditions.

Equations (15)-(18) are implemented in the *Modelica Text Layer*, while the look-up table is placed in the *Modelica Diagram Layer*, as shown in figure 11.

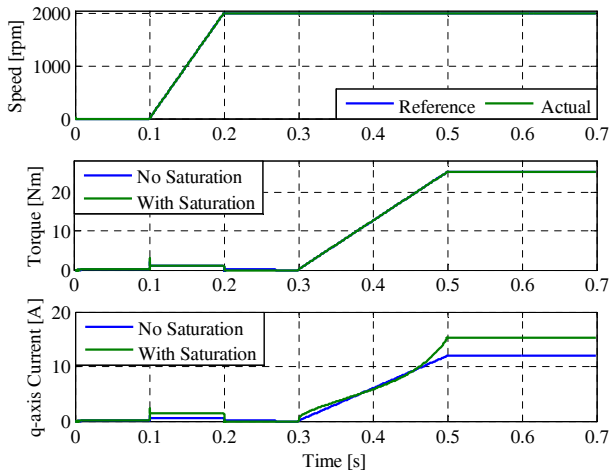


Figure 12: Simulation results obtained using the model Saturation under speed control: mechanical rotor speed (top), developed torque (middle) and  $q$ -axis current (bottom).

In order to verify the magnetic saturation influence on the PMSM performance, model Saturation has been simulated under speed control within Dymola. PMSM parameters are the same adopted for the simulation test shown in the previous section, while the magnetic saturation parameters are:

- $q$ -axis current at the knee equal to 5 A;
- field torque at the knee equal to 10.5 Nm;
- field torque in the saturated region equal to 30 Nm.

These parameters define the torque-current curve reported in figure 10 (blue line). During the simulation, the mechanical speed reference signal is a ramp from 0 rpm (at 0.1 s) to 2000 rpm (at 0.2 s), while the  $d$ -axis current reference signal is kept equal to 0 A. Once the speed reaches the demanded steady state value (2000 rpm), a load torque ramp from 0 Nm (at 0.3 s) to -25 Nm (at 0.5 s) is applied, in order to emphasize the magnetic saturation effect. Figure 12 shows the simulation results. In particular, the comparison between the  $q$ -axis currents flowing into the PMSM, with (green line) and

without magnetic saturation (blue line), is highlighted. When the magnetic saturation is considered, in order to develop the same electromagnetic torque (as in the absence of magnetic saturation), a higher  $q$ -axis current is required. Even during the acceleration phase, the  $q$ -axis current draw is higher when the magnetic saturation is taken into account. This is due to the analytical implementation of the torque-current curve (15). Indeed, torque-current curve is not a straight line in the linear region (see figure 10).

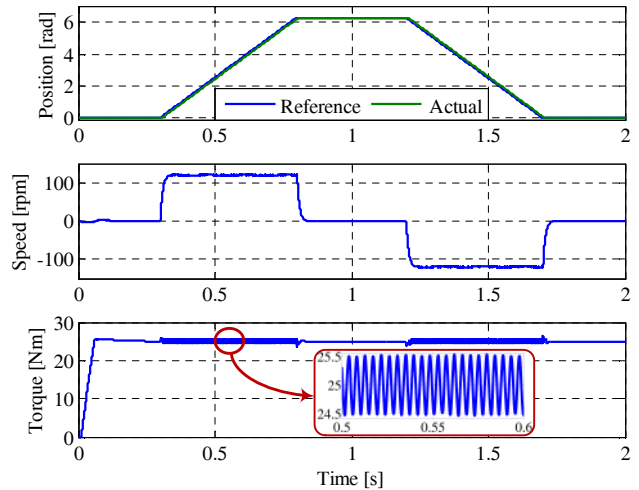


Figure 13: Simulation results obtained using the model Saturation under position control: mechanical rotor position (top), mechanical rotor speed (middle) and developed torque (bottom).

Figure 13 reports the simulation results obtained when the PMSM is position controlled and the torque ripple is considered. Torque ripple parameters have been set equal to 0.5 Nm amplitude (2% ripple) and 11200 Hz frequency. During the simulation, a -25 Nm load torque is applied. The enlargement in figure 13 (bottom plot) highlights the superimposition of the torque ripple on the developed torque. Torque oscillations, due to the ripple, have repercussions on both mechanical speed (middle plot) and  $q$ -axis current.

## 7 Models Fault

Models including fault conditions have been implemented only for PMSM (package Permanent-Magnet), since the presence of permanent magnets is the source of concern in the event of fault conditions. Indeed, fault condition is supplied by the back electromotive force due to the permanent magnets [9]. PMSM models including fault conditions have been implemented in the phase reference frame ( $abc$ ), since asymmetric faults are considered as well. Winding short-circuits, winding open-circuits and permanent magnet demagnetization are the three



fault conditions considered during the failure modeling. For each of the mentioned fault conditions a specific model has been developed, in order to keep low the model complexity. The realized models are listed below:

- model `ShortCircuit`, which implements single- and three-phase short-circuits;
- model `OpenCircuit`, which considers single- and three-phase open-circuits;
- model `Demagnetization`, which takes into account the permanent magnet demagnetization.

As suggested in [10], the winding faults have been implemented by means of ideal electrical switches. Such switches are driven by Boolean variables in order to open or close the phase windings and inject the fault conditions. Figures 14 and 15 show the *Modelica Diagram Layer* of model `ShortCircuit` and model `OpenCircuit` respectively.

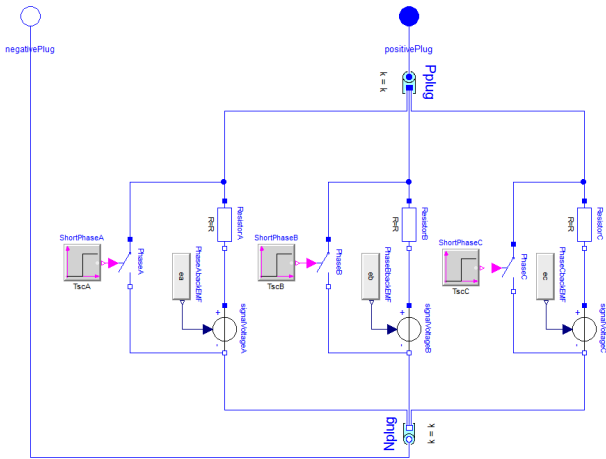


Figure 14: *Modelica Diagram Layer* of the model `ShortCircuit` included in the Electrical Machines library.

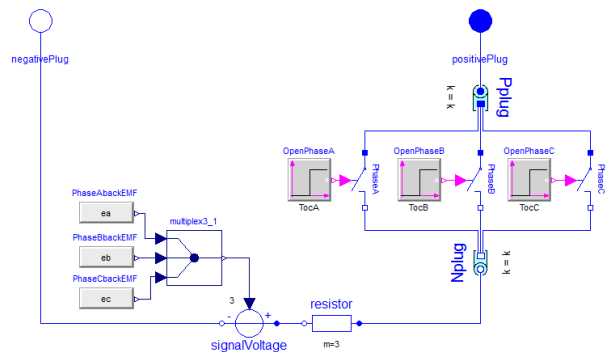


Figure 15: *Modelica Diagram Layer* of the model `OpenCircuit` included in the Electrical Machines library.

Demagnetization is caused by increasing of temperature inside the permanent magnet and/or high current values. In the model `Demagnetization`, the fault condition is considered as consequence of the fault

(i.e. permanent magnet flux reduction) neglecting the causes that led to the fault.

Figure 16 shows the Dymola block diagram used for testing the models including fault conditions. In particular, PMSM is current controlled (with  $i_q = 10 A$  and  $i_d = 0 A$ ) and its rotor is speed driven at a constant  $500 rpm$ . For the sake of brevity, only the simulation results regarding model `ShortCircuit` and model `OpenCircuit` are reported here. Moreover, the PMSM parameters are the same as those adopted in the model `Standard`, within section 5. Using model `ShortCircuit`, a three-phase short-circuit (symmetric fault) has been injected at  $0.3 s$ . By this time, the mechanical speed and currents have reached the steady state values. The corresponding simulation results are reported in figure 17. From the top plot, it is evident that the rotor speed is kept constant even after the fault injection. The middle plot shows the braking torque ( $T_{br}$ ) and its the steady state value is equal to  $-3.57 Nm$ . The same value can be obtained applying the formula reported in [11] and written below:

$$T_{br} = -\frac{3}{2} \cdot pp \cdot R \cdot \lambda_{PM}^2 \cdot \omega_e \cdot \frac{R^2 + \omega_e^2 \cdot L_q^2}{(R^2 + \omega_e^2 \cdot L_d \cdot L_q)^2} \quad (19)$$

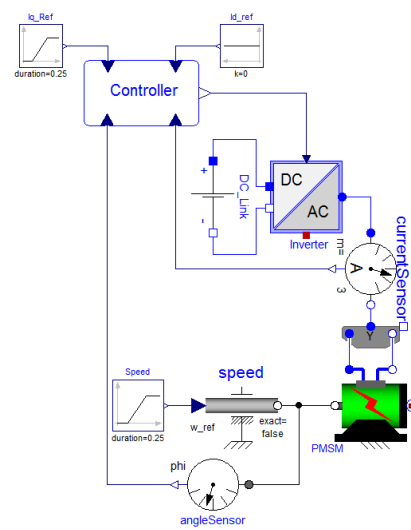


Figure 16: Block diagram implemented in Dymola, for testing both model `ShortCircuit` and `OpenCircuit`.

Since the three-phase short-circuit is a symmetric fault, the current components in the  $dq$  reference frame can be defined (see bottom plot). The steady state values of the  $dq$  current components are  $i_{qsh} = -1.7 A$  and  $i_{dsh} = -49.9 A$ . These values are in line with those obtained applying the analytical formulas reported in [11].

$$I_{dsh} = -\frac{\omega_e^2 \cdot \lambda_{PM} \cdot L_q}{R^2 + \omega_e^2 \cdot L_d \cdot L_q} \quad (20)$$

$$I_{qsh} = -\frac{\omega_e \cdot \lambda_{PM} \cdot R}{R^2 + \omega_e^2 \cdot L_d \cdot L_q} \quad (21)$$

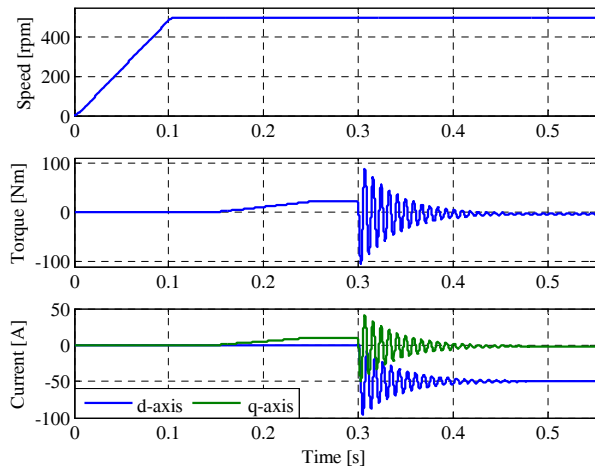


Figure 17: Simulation results obtained using the model `ShortCircuit`, in case of three-phase short-circuit: mechanical rotor speed (top), developed torque (middle) and  $dq$  currents (bottom).

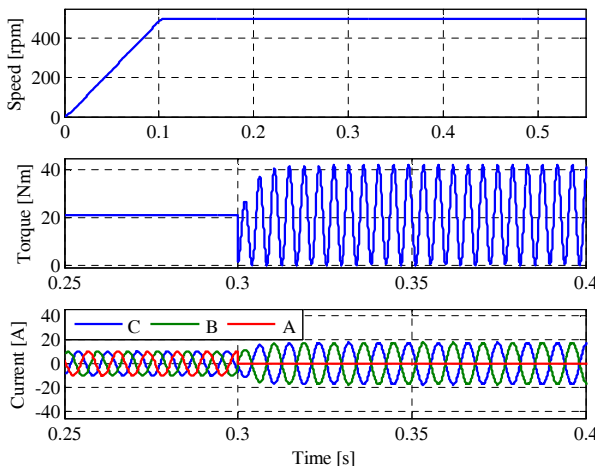


Figure 18: Simulation results obtained using the model `OpenCircuit` in case of single-phase open-circuit: mechanical rotor speed (top), developed torque (middle) and  $abc$  currents (bottom).

In figure 18, the simulation results obtained using model `OpenCircuit` are reported. In this case, a single-phase open-circuit (asymmetric fault) is injected into phase  $a$  at  $0.3$  s. After the fault injection, the developed torque (middle plot) becomes oscillating, since the PMSM currents are unbalanced. The pulsating torque component is shown alongside the demanded torque under healthy conditions ( $21$  Nm). Its frequency is twice the operating frequency of the PMSM. Since the stator winding is assumed wye-connected, with a floating neutral point, and the current in phase  $a$  is null, due to the

phase opening, the phase currents in phases  $b$  and  $c$  must be shifted by 180 degrees. The described situation can be observed in the bottom plot of figure 18.

## 8 Conclusions

An electrical machines library developed using Modelica has been presented in this paper. Particular attention has been paid to the PMSM models, since PMSMs are becoming widespread in aerospace applications, due to their inherent features. A multi-level approach has been adopted, in order to keep the model complexity low and reduce the computation time. The interchangeability among modelling levels has been ensured by using common interfaces. All the models are power balanced and can work as either a motor or generator. The main physical effects taken into account are losses, thermal behavior, magnetic saturation, torque ripple and fault conditions. Physical effects included in the models have been discussed and their implementation has been detailed. The effectiveness of the various modelling levels has been proven through simulation results obtained in several operating conditions.

## References

- [1] A. Boglietti, A. Cavagnino, A. Tenconi and S. Vaschetto, "The safety critical electric machines and drives in the MEA: A survey", in *IEEE Ind. Elec.*, Nov. 2009.
- [2] S.V. Bozhko, T. Wu, Y. Tao and G.M. Asher "MEA electrical power system accelerated functional modelling", in *Power Electr. and Motion Control*, Sep. 2010.
- [3] P. Fritzson, "Principles of Object-Oriented Modeling and Simulation with Modelica 2.1", IEEE Press, 2004.
- [4] J.F. Gieras "PM Motors Technology: Design and Applications", 3<sup>rd</sup> edition, Taylor and Francis, 2010.
- [5] C. Gerada and K.J. Bradley, "Integrated PM Machine Design for an Aircraft EMA", *IEEE Trans. on Ind. Elect.*, vol. 55, no. 9, pp.3300-3306, Sept. 2008.
- [6] R.H. Park, "Two-reaction theory of synchronous machines generalized method of analysis-part I", *Trans. of the American Institute of Electrical Engineers*, vol. 48, no. 3, pp. 716-727, July 1929.
- [7] N. Urasaki, T. Senjyu and K. Uezato "A Novel Calculation Method for Iron Loss Resistance Suitable in Modeling PMSMs" *IEEE Trans. on Energy Conversion*, vol. 18, no. 1, pp. 41-77, March 2003.
- [8] G. Ferretti, G. Magnani and P. Rocco, "Simulating permanent magnet brushless motors in Dymola", 2<sup>nd</sup> Modelica Conference, pp. 109-115, March 2002.
- [9] S. Khwan-on, L. de Lillo, L. Empringham, P. Wheeler, C. Gerada, N.M. Othman, O. Jasim, and J. Clare, "FT power converter topologies for PMSM drives in aerospace applications", 13<sup>th</sup> EPE, pp. 1-9, 8-10 Sept. 2009.
- [10] D. Winkler and C. Gühmann, "Modelling of Electrical Faults in IMs Using Modelica", 48<sup>th</sup> Scandinavian Conference on Simulation and Modeling, 2007.
- [11] N. Bianchi, M.D. Pr e and S. Bolognani, "Design of a fault-tolerant IPM motor for electric power steering", *IEEE Trans. on Vehicular Technology*, vol. 55, no. 4, pp. 1102-1111, July 2006.